Journal of Molecular Structure 920 (2009) 90–96

Contents lists available at ScienceDirect

Journal of Molecular Structure

journal homepage: www.elsevier.com/locate/molstruc

Linear free energy relationships of the ^{1}H and ^{13}C NMR chemical shifts in 3-cyano-4-(substituted phenyl)-6-phenyl-2(1*H*)pyridones

Aleksandar D. Marinković [a,*], Bratislav Ž. Jovanović [a], Nina Todorović [b], Ivan O. Juranić [c]

[a] Faculty of Technology and Metallurgy, University of Belgrade, Karnegijeva 4, 11120 Belgrade, PO Box 3503, Serbia
[b] Institute for Chemistry, Technology and Metallurgy, Njegoševa 12, 11000 Belgrade, Serbia
[c] Faculty of Chemistry, University of Belgrade, Studentski trg 12-16, P.O. Box 158, 11001 Belgrade, Serbia

ARTICLE INFO

Article history:
Received 11 September 2008
Received in revised form 11 October 2008
Accepted 17 October 2008
Available online 1 November 2008

Keywords:
3-Cyano-4-(substituted phenyl)-6-phenyl-2(1*H*)pyridones
LFER
Direct polarization
Extended polarization
Field effect

ABSTRACT

Linear free energy relationships (LFER) were applied to the ^{1}H and ^{13}C NMR chemical shifts in 3-cyano-4-(substituted phenyl)-6-phenyl-2(1*H*)pyridones. The correlation analysis for the substituent-induced chemical shifts (SCS) with inductive (σ_I), and various resonance (σ_R) parameters were carried out using SSP (single substituent parameter), DSP (dual substituent parameter), and DSP-NLR (dual substituent parameter non-linear resonance) methods, as well as by multiple regression analysis. The presented calculation accounts satisfactorily for the polar and resonance substituent effects operating at pyridone carbon atoms. Negative ρ values were found for several correlations (reverse substituent effect). The conformations of investigated compounds have been studied by the use of semi-empirical MO-PM6 method and B3LYP density functional (DFT) hybrid methods. The twist of the plane of 4-substituted phenyl ring (θ_1) is determined by electronic substituent effects, while the angles θ_2 are almost constant.

1. Introduction

The interest in various 3-cyano-4-substituted phenyl-6-phenyl-2(1*H*)-pyridone derivatives stems largely from their unique properties, which enable their use not only in the production of dyes, pigments, fuel and oil additives, but also for the development of medical products having a broad spectrum of biological activities.

An excellent review on the synthesis, reactivity and biological activity of 3-cyanopyridine-2(1*H*)-chalcogenones have been published [1]. Substances that improve the blood circulation and regulate cardiotonic activity have been mentioned as the most important. Among the other types of biological activities of the compounds of this class, it is worth mentioning analgetic and antihypertensive, antianaphylactic, diuretic and sodiodiuretic, antioxidant, antiviral, and antimicrobial compounds [1,2]. Biologically degradable agrochemical products, plant growth regulators, pesticides and herbicides are also produced from pyridone derivatives [3,4]. Considering the structural characteristics of 2-pyridones, existence of pyridone–pyridinol tautomerism, with the pyridone being dominant species in solution, and the group —NH—C(=O)—, similar to proteine amide bond, it was resonable to expect inherent physiological activity. This mostly depends on the activity of amide bond hydrogen which is highly influenced by tautomerism and resonance which in turn depend on the substituents on the pyridone ring. Therefore the study of the transmission of substituent electronic effects through investigated compounds could give better understanding of their structure–activity relationships.

The chemical shifts in ^{13}C and ^{1}H NMR spectra are frequently used for the study of the transmission of electronic effects of substituents in organic molecules. Analysis of both ^{13}C and ^{1}H NMR substituent chemical shifts (SCS) is based on the principles of linear free energy relationships (LFER) using the SSP and DSP equations in the form

$$SCS = \rho\sigma + h \quad (1)$$

$$SCS = \rho_I\sigma_I + \rho_R\sigma_R + h \quad (2)$$

where SCS are the substituent chemical shifts, ρ is the proportionality constant reflecting the sensitivity of the ^{13}C and ^{1}H NMR chemical shifts to substituent effects, σ is the corresponding substituent constant, and h is the intercept (*i.e.* describes unsubstituted member of series).

Eq. (1) attributes the observed substituent effect to an additive blend of polar and π-delocalization effects given as corresponding $\sigma_{o/m/p}$ values. In the dual-substituent parameter (DSP) Eq. (2) SCS are correlated by a linear combination of inductive (σ_I) and various resonance scales ($\sigma_R^0\sigma_R$ and σ_R^+) depending on the electronic demand of the atom under examination. Calculated values ρ_I and ρ_R are relative measures of the transmission of inductive and resonance effects through the investigated system.

* Corresponding author. Tel.: +381 11 3370416; fax: +381 11 3370387.
E-mail address: marinko@tmf.bg.ac.yu (A.D. Marinković).

0022-2860/$ - see front matter © 2008 Elsevier B.V. All rights reserved.
doi:10.1016/j.molstruc.2008.10.018

The dual substituent parameter non-linear resonance (DSP-NLR) analysis [5] is a successful method in modeling the long-range substituent effects on ^{13}C NMR substituent chemical shifts (in substituted aromatic systems [5–8]) that show deviations from the Hammett-type correlations. Need for different σ_R scales can be better accommodated by the use the (DSP-NLR) method developed by Bromilow et al. [5], which allows the resonance scale to vary with the electron demand of the site. This was achieved by the use parameter ε, characteristic of the group attached to the site, and an Eq. (3) in the form

$$SCS = \rho_I \sigma_I + \rho_R \sigma_R^{\circ}/(1 - \epsilon\sigma_R^{\circ}) + h \quad (3)$$

gives the best correlation of *para*-SCS in *p*-disubstituted benzenes [5], as well as in β-substituted styrenes [6], 3-phenyl and 3-thienyl-2-cyanoacrylamides [7] and *N*-1-*p*-substituted phenyl-5-methyl-4-carboxy uracils [8].

In the present study, linear free energy relationships (LFER) were applied to the ^{13}C and ^{1}H NMR chemical shifts in the 3-cyano-4-substituted phenyl-6-phenyl-2(1*H*)-pyridones, with the aim to get an insight into the factors determining chemical shifts in investigated compounds. The transmission of polar and resonance electronic effects in the investigated compounds (Fig. 1a), from the substituent (X) in the phenyl group to the carbon atoms of the pyridone, as well as to H(5) and N—H hydrogens, were studied by using Eqs. (1)–(3). Performed semi-empirical MO-PM6 calculations suggest that investigated pyridones prefer non-planar conformations. The contributions from both electronic substituent effects and the other factors that determine chemical shifts were discussed corresponding to such geometry. The most stable conformation of 3-cyano-4-(2-methoxyphenyl)-6-phenyl-2(1*H*)-pyridone is presented by structure in Fig. 1b).

2. Experimental

All 3-cyano-4-substituted phenyl-6-phenyl-2(1*H*)-pyridone derivatives were synthesized as described in the literature [9]. New compounds (6, 7, 11, 12, and 14) have satisfactory elemental analysis.

Structure of the studied compounds was confirmed using UV, IR, ^{13}C and ^{1}H NMR and MS data. IR Spectra were recorded on a Bomem MB 100 FTIR spectrophotometer in the form of KBr pellets. All mass spectra were recorded on a Thermo Finnigan Polaris Q ion trap mass spectrometer, including TraceGC 2000 (ThermoFinnigan Corp., Austin, TX, USA), integrated GC-MS/MS system.

The 1D ^{13}C and ^{1}H NMR spectral measurements were performed on a Varian Gemini 2000 (200 MHz). The spectra were recorded at room temperature in deuterated dimethyl sulfoxide (DMSO-d_6). The chemical shifts are expressed in ppm values referenced to TMS (δ_H = 0 ppm) in ^{1}H NMR spectra, and the residual solvent signal (δ_C = 39.5 ppm) in ^{13}C NMR spectra.

2D NOESY, HMBC and HSQC spectra were recorded on a Bruker DMX 500 spectrometer (500.13 MHz for ^{1}H, 125.77 MHz for ^{13}C) equipped with inverse detection triple resonance 5 mm probe (TXI). Standard pulse sequences were used for 2D spectra. 2D NOESY spectra were recorded at spectral widths of 5 kHz in both *F*2 and *F*1 domains; 1K × 512 data points were acquired with 32 scans per increment and the relaxation delays of 2.0 s. The mixing time in NOESY experiments was 1 s. Data processing was performed on a 1K × 1K data matrix. Inverse-detected 2D heteronuclear correlated spectra were measured over 512 complex points in *F*2 and 256 increments in *F*1, collecting 128 (HSQC) or 256 (HMBC) scans per increment with the relaxation delays of 1.0 s. The spectral widths were 5 and 27 kHz in *F*2 and *F*1 dimensions, respectively. The HMQC experiments were optimized for C—H couplings of 145 Hz; the HMBC experiments were optimized for long-range C—H couplings of 8 Hz. Fourier transform was done on a 512 × 512 data matrix. $\pi/2$ Shifted sine squared window functions were used along *F*1 and *F*2 axes for all 2D spectra.

2.1. Geometry optimization

The reported conformations of the molecular forms were obtained by semi-empirical MO PM6 method [10], with implicit DMSO solvation (COSMO) (Keywords: EF, GNORM = 0.01, EPS = 48, NSPA = 92 and LETDDMIN = 0.0) using the MOPAC2007™ program package. The VEGA ZZ 2.2.0 was used as the graphical user interface (GUI) [11].

3. Results and discussion

The chemical shifts (SCS) of the corresponding pyridone ring carbon atoms and H(5) and N—H hydrogens, are given in Table 1., in terms of the substituent chemical shifts (SCS) relative to the parent compound.

The SCS values in Table 1 indicate that substituents at the phenyl ring have a relatively small influence on the electron density at all pyridone ring carbon and hydrogen atoms. The reverse substituent effect is operative at C(2), C(5) for all substituents, at C(4) carbon for electron-acceptor and *ortho*-substituents, and at C(3) for *ortho*-substituents. Among factors contributing to the different SCS values (Table 1) the geometry of the investigated pyridones plays an important role arising from an out-of-plane rotation of phenyl rings for the torsion angles θ_1 and θ_2 (Fig. 1). Thus, a definite molecular geometry is deduced as a consequence of the particular

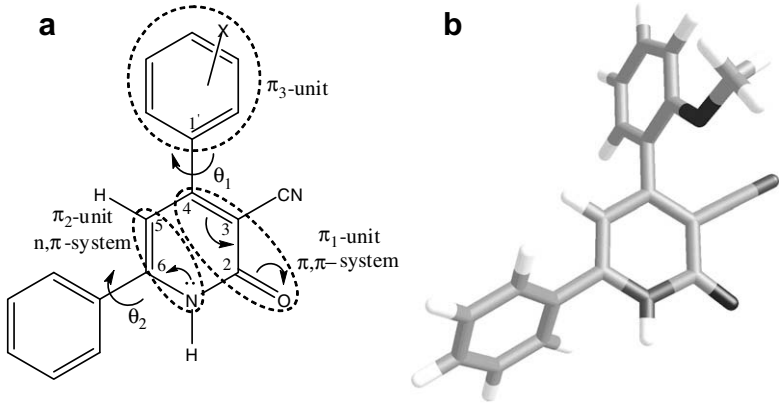

Fig. 1. Structure of the 3-cyano-4-substituted phenyl-6-phenyl-2(1*H*)-pyridones with labels of the nuclei under investigation and π-resonance units (a), and optimized conformation of 3-cyano-4-(2-methoxyphenyl)-6-phenyl-2(1*H*)-pyridone (b).

Table 1
SCS values of H(5-Pyr), N—H and pyridone carbon atoms of 3-cyano-4-substituted phenyl-6-phenyl-2(1*H*)-pyridones in DMSO-d_6[a].

No	X	H(5)	N-H	C(2)	C(3)	C(4)	C(5)	C(6)
1	H[b]	6.837	12.837	162.312	106.468	160.054	116.8	151.697
2	4-OMe	−0.034	−0.12	0.146	−0.255	−0.528	0.32	−0.474
3	4-Me	−0.056	−0.061	0.091	−0.164	−0.109	0.138	−0.237
4	4-Cl	0.015	0.032	−0.091	−0.109	−1.293	−0.281	0.20
5	4-Br	0.011	0.034	−0.091	−0.164	−1.22	−0.19	0.346
6	4-CN	0.067	0.111	−0.182	−0.072	−1.802	−0.445	0.637
7	4N[c]	0.105	0.168	−0.292	−0.028	−0.494	-0.372	1.313
8	4-NO_2	0.128	0.142	−0.430	−0.166	−2.300	−0.704	0.602
9	3-Me	−0.021	−0.005	0.018	−0.036	0.109	−0.044	−0.091
10	3-OCH_3	0.021	0.014	−0.01	0.013	−0.501	−0.433	0.009
11	3-OPh	0.021	−0.026	0.0	−0.072	−0.874	−0.172	0.203
12	3-Cl	−0.021	−0.008	−0.109	0	−1.675	−0.281	0.328
13	3N[d]	0.133	0.091	−0.182	0.019	−3.022	−0.281	0.51
14	3-NO_2	0.169	0.137	−0.182	0.164	−2.391	−0.408	0.71
15	2-OCH_3	−0.091	−0.055	−0.337	1.16	−3.978	−0.36	0.446
16	2-Cl	−0.001	0.156	−0.556	0.705	−1.702	−1.033	0.41
17	2-NO_2	0.104	0.155	−0.738	−0.387	−1.393	−1.124	0.483
18	2-Cl, 5-NO_2[e]	0.128	0.269	−0.683	0.614	−3.942	−1.215	1.138
19	2,4-di-Cl[f]	0.025	0.183	−0.673	0.583	−2.767	−1.118	0.673

[a] ^{13}C Chemical shifts (in ppm.) expressed relative to the unsubstituted compound, downfield shifts are positive.
[b] Chemical shifts of the unsubstituted compound relative to the TMS (^1H) and residual solvent signal at 39.5 ppm (^{13}C).
[c,d] 3- and 4-Pyridyl groups attached at 4-position of pyridone ring.
[e] 2-Chloro-5-nitro substituent.
[f] 2,4-Dichloro substituent.

transmission modes of the substituent electronic effects. Aromaticity study by NMR spectra indicated that 2-pyridones have approximately 35% of the benzene aromatic character [12], as defined by the ability to sustain an induced ring current, what could be ascribed to a definite non-planarity of 2-pyridone moiety interfering with the transmission mode of substituent effects.

To explain this observation, we applied the LFER analysis using SSP Eq. (1) and $\sigma_{o/m/p}$ values from the literature [13,14], with additive values for disubstituted compounds (18) and (19). The obtained results are given in Table 2.

The SSP correlation with Eq. (1) for $SCS_{C(3)}$ and $SCS_{C(5)}$ (electron-acceptors) are of poor precision, while all the others are good or excellent for $SCS_{H(5)}$ (for *ortho*-substituent) and $SCS_{C(3)}$ (for electron-donors), respectively (Table 2). The observed ρ values for both protons indicate different susceptibilities of their chemical shifts to substituent effects, the $SCS_{N—H}$ being more influenced.

According to the observed ρ values for all carbons, it is apparent that chemical shifts of C(4) show an increased susceptibility to substituent effects (particularly for electron-donating substituents) compared with other carbons. Statistically unacceptable correlation for C(5) carbon, is highly improved if $\sigma_{m/p}^+$ were used for 3N, 4N, 3-NO_2 and 4-NO_2 substituents, giving following correlation parameters for electron-withdrawing substituents: $\rho = -.620$; $r = 0.985$; sd = 0.09; $F = 25$ and $n = 10$.

It is generally assumed that substituent effect at the *ortho* position can be broadly classified as electronic, steric and anisotropic

Table 2
Correlations of the SCS values for investigated compounds with SSP equation.

No.		ρ	h	r[a]	sd[b]	F[c]	n[d]
H(5)	*ea* and *ed*	0.151 (±0.012)	−0.009 (±0.005)	0.965	0.016	160	14
	o	0.154 (±0.013)	−0.10 (±0.012)	0.991	0.013	164	5
N—H	*ea*, *ed* and *o*	0.220 (±0.016)	−0.031 (±0.010)	0.958	0.030	188	19
C(2)	*ea* and *ed*	−0.335 (±0.021)	0.024 (±0.011)	0.976	0.033	245	14
	o	−0.271 (±0.047)	−0.357 (±0.048)	0.965	0.053	33	5
C(3)[e]	*ed*	0.990 (±0.090)	0.012 (±0.014)	0.992	0.018	124	4
	o	−0.770 (±0.110)	1.270 (±0.17)	0.977	0.130	60	5
C(4)	*ed*[f]	3.185 (±0.580)	0.365 (±0.109)	0.984	0.082	30	3
	ea and *o*[g]	−2.985 (±0.313)	−0.221 (±0.191)	0.944	0.370	90	13
C(5)	*ed*[h]	−1.909 (±0.327)	−0.174 (±0.047)	0.946	0.110	34	6
	ea	−0.502 (±0.10)	−0.053 (±0.055)	0.872	0.090	25	10
	o	−0.414 (±0.044)	−0.744 (±0.041)	0.989	0.014	88	4
C(6)	*ea* and *ed*	1.120 (±0.064)	−0.064 (±0.022)	0.985	0.064	302	11
	o	1.144 (±0.115)	−0.403 (±0.102)	0.971	0.115	97	8[i]

[a] Correlation coefficient.
[b] Standard error of estimate.
[c] *F*-test for significance of regression.
[d] Number of points.
[e] Correlation for electron-acceptor is not of statistical value.
[f] Without H.
[g] Without 2-OCH_3, 2-NO_2, 4-NO_2 and 4N.
[h] Including 2-OCH_3 and 3-OCH_3.
[i] Including 4-NO_2, 3N and 4N. *ea* designate electron-acceptor, *ed* electron-donor and *o* *ortho*-subtituents.

Table 3
Correlation of the SCS values for investigated compounds with DSP equation.

	Scale[a]		ρ_I	ρ_R	h	r	sd	F	n	λ[b]	f[c]
H(5)	σ_R	*ed* and *ea*	0.155 (±0.017)	0.157 (±0.026)	−0.011 (±0.008)	0.975	0.015	94	14	1.01	0.208
		o	0.192 (±0.042)	0.271 (±0.081)	−0.154 (±0.034)	0.972	0.029	17	5	1.41	0.341
N—H	σ_R	*ed*, *ea* and *o*	0.180 (±0.027)	0.296 (±0.043)	−0.012 (±0.015)	0.961	0.030	97	19	1.64	0.159
C(2)	σ_R	*ed* and *ea*	−0.297(±0.044)	−0.391 (±0.048)	0.011 (±0.020)	0.974	0.037	99	14	1.32	0.253
		o	−0.348 (±0.050)	−0.266 (±0.047)	−0.32 (±0.038)	0.988	0.035	41	5	0.76	0.056
C(3)[d]	σ_R	*ed*	0.703 (±0.164)	1.058 (±0.148)	0.007 (±0.012)	0.996	0.018	58	4	1.50	0.117
		o	−0.490 (±0.096)	−0.863 (±0.054)	1.093 (±0.075)	0.994	0.068	139	5	1.76	0.092
C(4)	σ_R	*ed*	2.262 (±0.780)	1.332 (±0.133)	0.183 (±0.102)	0.991	0.169	55	4	0.59	0.177
		ea and *o*	−3.441 (±0.320)	−1.528 (±0.650)	−0.026 (±0.200)	0.965	0.308	69	13[e]	0.44	0.149
C(5)	σ_R	*ed*	−2.284 (±0.530)	−2.248 (±0.532)	−0.156 (±0.080)	0.935	0.131	11	6[f]	0.98	0.346
		ea	−0.605 (±0.161)	−0.360 (±0.218)	−0.001 (±0.085)	0.887	0.880	13	10	0.59	0.980
		o	−0.392 (±0.056)	−0.345 (±0.107)	−0.770 (±0.056)	0.992	0.016	34	4	0.88	0.105
C(6)	σ_R	*ed* and *ea*	1.034 (±0.104)	1.447 (±0.172)	0.013 (±0.046)	0.979	0.080	95	11	1.39	0.130
		o	1.350 (±0.200)	0.579 (±0.194)	−0.541 (±0.144)	0.965	0.137	34	8[g]	0.43	0.201

[a] σ_I and σ_R are from Refs. [13,14].
[b] $\lambda = \rho_R/\rho_I$.
[c] Taft f value, f = sd/rms (rms-root mean square value).
[d] Correlation for electron-acceptor is not of statistical value.
[e] Without 2-OCH_3, 2-NO_2, 4-NO_2 and 4N.
[f] Including 2-OCH_3.
[g] Including 4-NO_2, 3N and 4N.

[15,16], two former being the most significant, since anisotropic effect makes a relatively small contribution to ^{13}C NMR chemical shifts. The anisotropy effect depends on spatial arrangement, but it is independent of the nuclei being observed [17]. Steric effect includes all those phenomena which result in conformational influence at the measured sites, such as bond lengths and angles, effects due to size of the *ortho*-substituents. The diamagnetic anisotropy effect of the *ortho*-substituted phenyl group could contribute to $SCS_{H(5)}$, but no to $SCS_{N—H}$, while the later is more sensitive to substituent effects, probably due to its *para*-position to 4-substituted phenyl group.

Although SSP analysis uses an additive blend of inductive and resonance parameters of substituents given as $\sigma_{o/m/p}$ values, it presented a satisfactory description of substituent electronic effects in correlation Eq. (1). To measure separate contributions of polar (inductive/field) and resonance effects of substituent (X), the regression analysis according to Eq. (2), DSP analysis, with σ_R^0, σ_R, σ_R^+ substituent constants [13,14,18] was carried out, and the results of the best fit are given in Table 3.

Results of DSP fits are similar to or slightly better than SSP correlations. The observed ρ_I and ρ_R values for H(5) and N—H protons indicate a somewhat higher contribution resonance effect at amide hydrogen. Owing to the particular geometric arrangement of the carbons in pyridone unit (see Fig. 1), both regression coefficients should have different sensitivities to polar and resonance effects [19]. This is consistent with the different magnitudes of observed ρ_I and ρ_R values for all carbons. Generally, polar effect is more important effect, except for $SCS_{C(2)}$ and $SCS_{C(6)}$ (electron-donors and -acceptors), and $SCS_{C(3)}$ for all substituents (Table 3). In other word, chemical shifts of the carbons of interest reflect distance/angle dependence of field effect as well as path-length/pathway dependence of the inductive σ effect. The alternation of polar substituent effects have been manifested as variation of the values of ρ_I coefficients in Table 3. The extent of observed alternation bears evidence for the transfer of substituent effects by the bond-polarization mechanism. This is particularly apparent for the carbons where ρ_I are negative and significantly higher compared to ρ_R values. Transmission of the resonance effect strongly depends on the non-planar molecular geometry of the investigated compounds (see Fig. 1.).

Resonance effect has significant contribution for some carbon atoms in molecule, which proves that the demand for electrons of the carbon atoms of investigated compounds are significantly different, therefore the used σ_R scales cannot adequately describe resonance effect of substituent on these carbon atoms. We performed the correlations of the SCS values for pyridone derivatives

Table 4
Correlations of the SCS values for the investigated compounds with DSP-NLR equation.

		ρ_I	ρ_R	h	ε	r	sd	F	n	λ	f
H(5)	*ea* and *ed*	0.150 (±0.012	0.147 (±0.014)	−0.014 (±0.005)	−0.16	0.989	0.010	244	13[a]	0.98	0.157
N—H	*ea* and *ed*	0.198 (±0.014)	0.267 (±0.009)	0.008 (±0.007)	−0.65	0.997	0.014	918	13[b]	1.35	0.076
C(2)	*ea* and *ed*	−0.289 (±0.038)	−0.375 (±0.020)	0.002 (±0.017)	−0.64	0.992	0.033	297	12[c]	1.30	0.147
C(4)	*ea* and *o*	−3.459 (±0.190)	−3.270 (±0.453)	−0.084 (±0.117)	−1.75	0.990	0.184	198	10[d]	0.94	0.086
C(5)	*ea*	−0.612 (±0.051)	−0.486 (±0.043)	−0.013 (±0.025)	–	0.992	0.028	210	9[e]	0.79	0.078
C(6)	*ea* and *ed*	0.967 (±0.118)	1.337 (±0.106)	−0.035 (±0.051)	–	0.988	0.096	245	13[f]	1.38	0.156

[a] Without 3N.
[b] Without 3N.
[c] Without 4N and 3-OPh.
[d] Without 2-OCH_3, 2-NO_2, 4-CN and 4N.
[e] DSP correlation: $\sigma_{m/p}^+$ for 3N, 4N, 3-NO_2 and without 4-NO_2.
[f] DSP correlation: σ_p^- for 3N and 4N, without 4-NO_2.

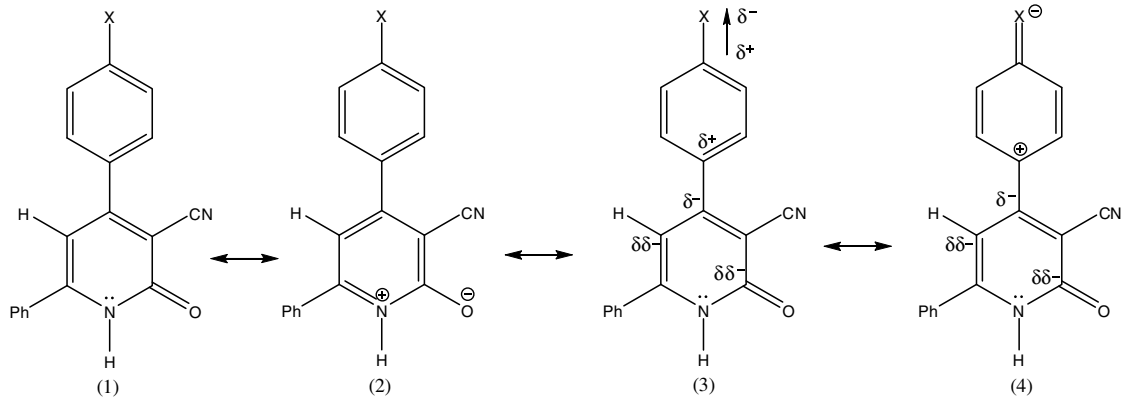

Fig. 2. Mesomeric structures of electron-acceptor substituted compounds with contribution of π-polarization.

according to the method of Bromilow et al. [5], to determine electronic demand of carbon atoms, applying DSP-NLR analysis, and results are given in Table 4.

Results from Table 4 shows that as good as DSP or much better correlations of SCS of some carbon atoms are obtained using DSP-NLR Eq. (3). Generally, on the basis of the above results can be concluded that two opposite effects, substituent electronic effects in phenyl ring and electronic interactions in the pyridone part of the molecule are balanced giving an overall effect on the chemical shifts of all carbon atoms. The calculated ρ_I and ρ_R values from Table 4 indicates prevalent polar (inductive/field) effect on the C(5). It can be noted that ρ_I and ρ_R are negative for C(2), C(4), and C(5), while those for other carbon atoms are positive. A negative sign of ρ_I is indicative of the reverse SCS effect, *i.e.*, inductive electron-acceptor substituents cause an upfield shift, which has been explained to be due to π-polarization [20]. Similar effect have been observed in other systems, in *N*-1-*p*-substituted phenyl-5-methyl-4-carboxy uracils [8], 3-aryl-2-cyanoacrylamides [21], *N*-benzylidenanilines [22], 2-substituted-5-*N*′,*N*′-dimethy-laminophenyl-*N*,*N*-dimethyl carbamates [23], and in the other systems containing a conjugated side chain.

As cited in the literature, π-polarization of a distant π-system by substituent dipole need not to be transmitted *via* an intervening π-system [20], and theoretical results have demonstrated that a substituent dipole acts mainly in polarizing each of the π-units individually [24], defined as "localized polarization" (direct π-polarization). On the other hand, the terminal atoms of a conjugated π-system show some additional polarization of the whole π-network. This component is termed "extended polarization".

Transmission of substituent electronic effects could be presented by mesomeric structures of the electron-acceptor substituted pyridones with contribution of π-polarization (Fig. 2).

In structure (1), if X is an electron-acceptor substituent, a dipole on X (or near the C—X bond) is induced (structure 3), and interaction of this dipole through molecular cavity results in the polarization of individual π-units (localized polarization). Polarization mechanism of small localized π-units, presented by structures (3 and 4), is very important, while polarization of the entire conjugated system of investigated compounds contribute to some extent (extended polarization). Resonance interaction in extended conjugated system of pyridone ring (structure 2) has an opposite effect to the polarization caused by electron-acceptor substituent (structure 4). The net result is that the electron-acceptor substituents increase the electron density on C(2), C(4), and C(5) carbons, hence, an increase in the shielding. Resonance interaction strongly depends on spatial arrangement of in molecules (see Table 5. θ_1 angles), and could be effectively transmitted by resonance to C(1′) carbon.

Interaction of π_1- and π_3-units could be analyzed on the basis of a novel here defined π-system containing π_3-unit and C(3)—C(4)

Table 5
Elements of optimized geometry of structures of 3-cyano-4-substituted phenyl-6-phenyl-2(1*H*)-pyridones by semi-empirical MO-PM6 method.

No.	Torsion angles		Interatomic distances						
	θ_1	θ_2	N(1)—C(2)	C(2)—C(3)	C(3)—C(4)	C(4)—C(5)	C(5)—C(6)	C(6)—N(1)	C(4)—C(1′)
1	119.7	126.7	1.4359	1.4472	1.3988	1.4113	1.3876	1.3850	1.4800
2	125.2	126.4	1.4345	1.4466	1.4009	1.4137	1.3861	1.3856	1.4730
3	123.2	126.4	1.4355	1.4468	1.4001	1.4128	1.3866	1.3855	1.4730
4	117.8	126.9	1.4365	1.4476	1.3982	1.4100	1.3866	1.3843	1.4808
5	116.3	126.9	1.4366	1.4477	1.3978	1.4094	1.3889	1.3841	1.4818
6	113.3	127.1	1.4370	1.4481	1.3971	1.4083	1.3898	1.3836	1.4839
7	109.8	127.2	1.4374	1.4484	1.3963	1.4071	1.3906	1.3831	1.4854
8	104.2	127.2	1.4378	1.4487	1.3959	1.4061	1.3914	1.3826	1.4867
9	118.5	126.8	1.4359	1.4474	1.3982	1.4110	1.3877	1.3850	1.4822
10	113.9	126.9	1.4364	1.4479	1.3969	1.4091	1.3890	1.3843	1.4859
11	115.4	126.7	1.4367	1.4479	1.3971	1.4087	1.3894	1.3839	1.4850
12	116.7	127.0	1.4366	1.4479	1.3975	1.4092	1.3891	1.3840	1.4828
13	119.9	126.9	1.4369	1.4476	1.3987	1.4099	1.3889	1.3838	1.4761
14	115	127.3	1.4375	1.4482	1.3973	1.4079	1.3902	1.3832	1.4822
15	89.5	127.3	1.4379	1.4463	1.3998	1.4101	1.3886	1.3841	1.4755
16	118.4	131.6	1.4360	1.4476	1.3974	1.4102	1.3895	1.3845	1.4790
17	87.8	127.2	1.4371	1.4483	1.3959	1.4074	1.3903	1.3836	1.4886
18	99.63	127.5	1.4382	1.4483	1.3964	1.4058	1.3915	1.3825	1.4832
19	118.9	132.3	1.4369	1.4478	1.3973	1.4097	1.3902	1.3843	1.4794

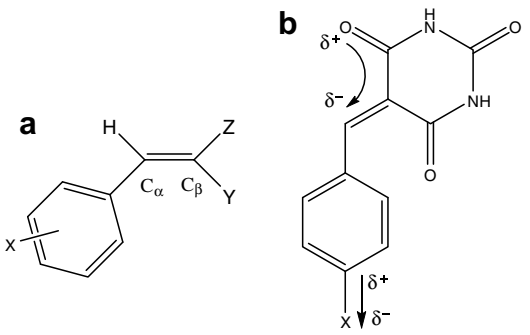

Fig. 3. Side chain SCS in styrene derivatives (a) and contribution of extended π-polarizaton in arylidenbarbituric acids (b).

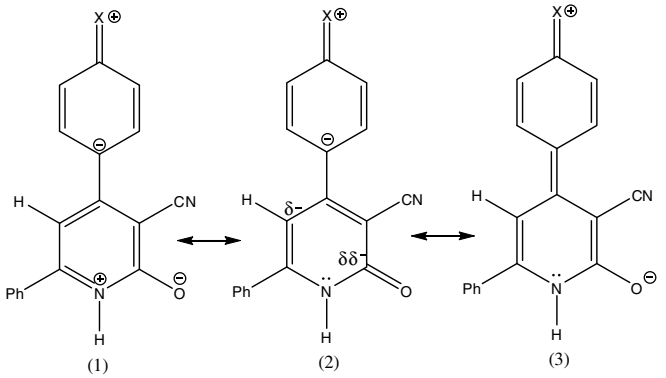

Fig. 4. Mesomeric structures of electron-donor substituted compounds with contribution of π-polarization.

double bond. SCS in similar systems (Fig. 3a) with conjugated side chain as in substituted styrenes [25], *meta* and *para*-substituted *trans*-cinnamonitriles [26] and *para*-substituted *cis*-cinnamonitriles [27] confirm dominance of resonance effect at C_{β}, while reverse polarization is operative at C_{α} Similar trend of substituent effects on SCS, with dominant resonance effect was noticed at C(3) for electron-donor and *ortho*-substituents, while reverse polarizations from electron-acceptor and *ortho*-substituents were operative at C(4) carbon. Contribution of polar effect is significantly increased at C(4) carbon, showing that conjugative group at C(3) carbon increases the magnitude of the ρ_I value, and higher increase is evident with electron-accepting substituents. This observation is consistent with increased extended polarization in π_1-unit caused by substituent dipole which induces transfer of electron density from terminal atom of the side-chain to the C(4) carbon. Increased ρ_I value for a site similar to C(4), has been also observed in the conjugated system of arylidenbarbituric acids [28], containing *cis*-π-enone unit, which illustrates the additional polarization in the corresponding conjugated system (Fig. 3b), described by the following equation: $SCS_{C\alpha} = -4.4\sigma_I - 1.7\sigma_R^-$; $f = 0.24$.

Geometry optimization of investigated systems in the present work shows significant deviation of substituted phenyl ring (Table 5.). Induced dipole, either on X or at whole substituted phenyl ring probably electrostaticaly interacts through the space with carbons in the molecule. Therefore contribution of a direct through space field effect must be rather significant. Repulsion of positively charged orbital of two aromatic π-electron systems causes additional contribution to that deviation. Manifestation of these effects influences large differences in ρ_I values for C(3), C(4), and C(5) atoms, which are affected by the substituent dipole to higher extent. Geometry optimization of some 4-substituted (4-NO_2, 4-OCH_3 and 4-Cl) and *ortho*-substituted compounds (2-NO_2, 2-OCH_3 and 2-Cl), using *ab initio* DFT(B3LYP) method, LanL2DZ and STO/6-311**G++ basis sets, shows positive net atomic charges at both carbons, significantly higher at C(4). *ortho*-Substituents by adjustment of the orientation of its dipole, could through the space electrostatically stabilize surrounding positive charges, with their negative end of dipole. Alternatively, in the case of 2-methoxy substituted compound, non-bonded oxygen π-orbital might cause strong stabilization of positive charges at both carbons. It is expected for such systems that substituent field effect could cause perturbation of π-electron density of pyridone ring which is reflected in π-electron shifts without direct interaction of the two systems.

The same trend of substituent effects was observed for electron-donor and electron-acceptor substituted compounds, except for C(4) carbon. Opposite directions at C(4) (V shape correlation) means that this break-point reflects different transmission mode of substituent electronic effects. Transmission of electron-donors substituent electronic effects could be presented by mesomeric structures of pyridones with a contribution of π-polarization (Fig. 4).

As defined by MO calculations (HOMO orbitals), electron-donors strongly polarize 4-phenyl ring, increasing electron-density at 4-substituted phenyl ring which therefore acts as a π-donor. Electron-donor substituents interfere with resonance interaction in the pyridone unit, supporting resonance interaction in enone π_1-unit and suppressing contribution of *n*, π-conjugation in π_2-unit. On the other side, deshielding effect of electron-donor at C(5) is indeed a type of a "push-effect" of electron rich phenyl ring, reflected through increased electron density at C(6) carbon.

Additional support for understanding of the investigated molecules could be obtained from their optimized geometries presented in Table 5.

The optimized conformations of investigated compounds are in a very good concordance with conformations derived from NOESY spectra. Established atom connectivity between H(5) proton and *ortho*-protons of 4-phenyl and 6-phenyl rings for 3- and 4-substituted compounds unambiguously confirm twisted orientation of the 4-substituted phenyl, as well as of 6-phenyl rings. Spatial relationships of two pairs of *ortho*-hydrogens with H(5) hydrogen from NOESY spectra are in good accordance with interatomic distances of those atoms taken from their optimized geometries. Valuable information have been obtained from 2D NOESY spectra of 2-methoxysubstituted compounds which show strong correlation peak of OCH_3 with meta hydrogen, which undoubtedly confirms the optimized geometry of that compound (see Fig. 1 b). The torsion angle θ_2 is approximately constant for all compounds, thus the small influence of 6-phenyl ring could be accepted to be constant. The values of torsion angles θ_1 depend on substituent present, preffering the perpendicular position for strong electron-acceptor and *ortho*-substituents. Transmission of the resonance effect from substituted phenyl ring is efficiently suppressed in this way. Calculated bond lengths clearly demonstrate longer C(4)—C(1′), C(3)—C(4), C(5)—C(6), and N(1)—C(2) bonds (Table 5) for all electron-acceptor substituted compounds, in that way helping to visualize the electron-densities distribution at 2-pyridone ring for those compounds. Generally, an electron-acceptor attracts electron density from pyridone ring, π-conjugation of enone system is suppressed while enhancement of *n*, π-conjugation contributes to higher electron density at C(5) carbon. Opposite is true for electron-donor substituted compounds.

Understanding the transmission of substituent electronic effect by π-polarization mechanism through differently oriented pyridone π-units was one of the goals of the present investigation. Dielectric properties of molecular framework will modify the electric field transmission of polarization effects. That means that

polarization effect is not necessarily transmitted in a direct line from a substituent to the probe sites. In that way different substituents cause different sensitivities reflected in the values λ and electron demands ε of the particular carbon atoms.

Somewhat lower demand for electrons ($\varepsilon = -.64$) was observed for C(2) atom of the pyridone ring. Polarizability of the π-carbonyl electrons is influenced by vicinity of electron-accepting oxygen. The ρ_I component appears to be mainly controlled by π-polarization mechanism. Ability of carbonyl group to conjugate causes a higher polarizability of π_1-enone unit and thus decreased demand for electron of this carbon. Similar literature value [5] of ε for CHO group (−0.60) proves that the electron density of pyridone ring is shifted to the carbonyl group depending on the substituent present.

The highest demand for electrons ($\varepsilon = -.75$) is observed for C(4) carbon for electron-acceptors and *ortho*-substituents. Higher sensitivity to substituent effects, comparing to C(4), shows C(1′) carbon, according to the following correlation result: $\rho = 9.803$; $r = 0.978$; sd = 1.039; $F = 270$ and $n = 14$, and DSP analysis: $\rho_I = 10.321$ and $\rho_R = 12.427$; $r = 0.979$; sd = 1.069; $F = 128$ and $n = 14$. Electron-donor substituted compounds show positive value of ρ_I and ρ_R for C(4) carbon, while those are negative for electron-acceptor substituents. Normal substituent effect was observed for C(1′) carbon, indicating that substituents in different way influence π-electron densities at those neighboring carbons. For C(4) carbon $\rho_I > \rho_R$, both for electron-donors and electron-acceptors (Table 2.), but oppositely is true for C(1′), $\rho_R > \rho_I$. The significantly decreased transmission of resonance effect to C(4) carbon is undoubtedly caused by non-planarity of substituted phenyl and pyridone rings. Less decreased but still high attenuation of the polar effect is not only affected by distance between individual π-units, but also by contribution of non-planarity of the system which influences the degree of the through-space transmission of the field effect.

DSP Correlations for C(5) and C(6) carbons were better than DSP-NLR, indicating that literature σ_R values give good description of substituent resonance effect. Results from Table 4. indicate that π-polarization mechanism is operative at C(5) carbon, while resonance effect significantly contributes at C(6) carbon. *ortho*-Substituent cause higher shielding, comparing to electron-acceptor, at both carbons in π_2-unit, N—H and H(5) hydrogens, together with consideration of C(4)—C(5), C(5)—C(6), and C(6)—N(1) bond lengths indicate that π_2-unit behaves as a isolated fragment to some extent.

4. Conclusion

Applied LFER analysis appears to be a straightforward method for correlations of SCS values of investigated molecules with appropriate substituent constants. All correlations are of good quality indicating that substituent effects on SCS are electronic in origin. Polar effect (inductive/field) and resonance effect have different contributions at all carbons. Because of the non-planarity of 4-substituted phenyl ring and pyridone ring, the transmission of resonance substituent effect is significantly decreased. Regardless on that observation and dependence of that effect on coplanarity of the double bonds, contribution of resonance effect at N—H, C(3) and C(6) is a dominant, which probably could be a manifestation of a "field transmitted resonance". Polar effect is the most prominent at other carbons, transmitted mainly by inductive, through space field effect and by π-polarization mechanism. Reverse polarization is operative at C(2) and C(5) carbons for electron-donors and electron-acceptors, and at C(4) for electron-acceptors and *ortho*-substituent, as a consequence of π-polarization. Regarding optimized geometries of investigated compounds and transmission of individual substituent electronic effects through a number of well defined π-resonance units, indicate that these units behaves either as isolated or conjugated fragments depending on substituents present in the corresponding molecule.

Acknowledgements

This work was supported by the Ministry of Science and Technological Development of Serbia (Project Nos. 142063 and 142010).

References

[1] V.P. Litvinov, S.G. Krivokolysko, V.D. Dyachenko, Chem. Heterocyclic Comp. 35 (1999) 509.
[2] M.C. Seidel, K.L. Viste, R.Y. Yih, US Patent 3.503.986 (1970).
[3] M.C. Seidel, K.L. Viste, R.Y. Yih, US Patent 3.576.814 (1971).
[4] M.C. Seidel, K.L. Viste, R.Y. Yih, US Patent 3.761.240 (1973).
[5] J. Bromilow, R.T.C. Brownlee, D.J. Craik, M. Sadek, R.W. Taft, J. Org. Chem. 45 (1980) 2429.
[6] S. Datta, A. De, S.P. Bhattacharyya, C. Medhi, A.K. Chakravarty, J.S.A. Brunskill, S. Fadoujou, K. Fish, J. Chem. Soc. Perkin Trans. II (1988) 1599.
[7] S.P. Bhattacharyya, A. De, A.K. Chakravarty, J.S.A. Brunskill, D.F. Ewing, J. Chem. Soc. Perkin Trans. II (1985) 473.
[8] F.H. Assaleh, A.D. Marinković, B.Ž. Jovanović, J. Csanádi, J. Mol. Struct. 833 (2007) 53.
[9] D. Mijin, A. Marinković, Synth. Commun. 36 (2006) 193.
[10] J.J.P. Stewart, J. Mol. Mod. 13 (2007) 1173–1213. Version 7.295.
[11] A. Pedretti, L. Villa, G. Vistoli, J. Comput. Aid. Mol. Des. 18 (2004) 167; VEGA ZZ 2.1.0. Available from: <http://www.ddl.unimi.it>.
[12] J.A. Elvidge, L.M. Jackman, J. Chem. Soc. (1961) 859.
[13] C. Hansch, A. Leo, R.W. Taft, Chem. Rev. 91 (1991) 165.
[14] C. Hansch, A. Leo, D. Hoekman, Exploring QSAR ACS Professional Reference Book, American chemical Society, Washington, DC, 1995.
[15] F. Membrey, J. Duvernoy, Spectrochim. Acta A 41 (1985) 65.
[16] D.J. Craik, B. Ternai, Org. Magn. Reson. 15 (1981) 268.
[17] S. Klod, E. Kleinpeter, J.Chem.Soc. Perkin Trans. II (2001) 1893.
[18] S. Ehrenson, R.C.T. Brownlee, R.W. Taft, Prog. Phys. Org. Chem. 10 (1973) 1.
[19] N.V. Valentić, G.S. Uščumlić, J. Serb. Chem. Soc. 68 (2003) 67.
[20] J. Bromilow, R.T.C. Brownlee, D.J. Clark, P.R. Fiske, J.E. Rowe, M. Sadek, J. Chem. Soc. Perkin Trans. 2 (1981) 753.
[21] S.P. Bhattaharya, A. De, A.K. Chakravarty, J.S.A. Brunskill, D.F. Ewing, J. Chem. Soc. Perkin Trans. II (1985) 473.
[22] R. Akaba, H. Sakuragi, K. Tokumaru, Bull. Chem. Soc. Jpn. 58 (1985) 1186.
[23] R. Rittner, J.E. Barbarini, N.F. Höehr, Can. J. Anal. Sci. Spectrosc. 44 (1999) 180.
[24] R.T.C. Brownlee, D.J. Craik, J. Chem. Soc. Perkin Trans. II (1981) 760.
[25] E.M. Shulman, K.A. Christensen, D.M. Grant, C. Walling, J. Org. Chem. 39 (1974) 2686.
[26] G. Butt, R.D. Topsom, Spectrochim. Acta 36A (1980) 811.
[27] G. Butt, R.D. Topsom, Spectrochim. Acta 38A (1982) 301.
[28] C.N. Robinson, C.C. Irving Jr., J. Heterocyclic Chem. 16 (1979) 921.